ELSEVIER

Journal of Structural Geology 29 (2007) 1709–1720

JOURNAL OF STRUCTURAL GEOLOGY

www.elsevier.com/locate/jsg

Methods for quantitatively determining fault slip using fault separation

S.-S. Xu [a,*], L.G. Velasquillo-Martínez [a], J.M. Grajales-Nishimura [a], G. Murillo-Muñetón [a], A.F. Nieto-Samaniego [b]

[a] *Instituto Mexicano del Petróleo Eje Central Lázaro Cárdenas Nort 152, Col. San Bartolo Atepehuacán, C.P. 07730 México, D.F., Mexico*
[b] *Universidad Nacional Autónoma de México, Centro de Geociencias, Apartado Postal 1-742, Querétaro, Qro. 76001, Mexico*

Received 23 February 2006; received in revised form 31 May 2007; accepted 10 June 2007
Available online 5 July 2007

Abstract

Fault slip and fault separation are generally not equal to each other, however, they are geometrically related. The fault slip (S) is a vector with a magnitude, a direction, and a sense of the movement. In this paper, a series of approaches are introduced to estimate quantitatively the magnitude and direction of the fault slip using fault separations. For calculation, the known factors are the pitch of slip lineations (γ), the pitch of a cutoff (β), the dip separation (S_{md}) or the strike separation (S_{mh}) for one marker. The two main purposes of this work include: (1) to analyze the relationship between fault slip and fault separation when slickenside lineations of a fault are known; (2) to estimate the slip direction when the parameters S_{md} or S_{mh}, and β for two non-parallel markers at a place (e.g., a point) are known. We tested the approaches using an example from a mainly strike-slip fault in East Quantoxhead, United Kingdom, and another example from the Jordan Field, Ector County, Texas. Also, we estimated the relative errors of apparent heave of the normal faults from the Sierra de San Miguelito, central Mexico.

Keywords: Fault; Fault slip; Fault separation; Method

1. Introduction

According to Reid et al. (1913) and Tearpock and Bischke (2003), fault displacement is a general term for fault movement and describes the relative movement of two rock blocks along the fault plane measured in any specified direction. This concept is the same as defined by Walsh and Watterson (1988). They consider that displacement refers to the displacement accumulation through the active period of a fault. Displacement also represents the variation in position of a marker displaced by the fault movement (Tearpock and Bischke, 2003). On the other hand, the fault slip can be visualized as the actual distance between two originally contiguous points on the two sides of a fault (e.g., Bates and Jackson, 1987; points B and B′ in Fig. 1). Furthermore, the fault separation is an apparent displacement between the displaced parts of a marker measured along a specified line (Hill, 1959). Dip separation (S_{md}) involves displacement parallel to the dip of a fault (EC′ in Fig. 1), whereas strike separation (S_{mh}) implies the displacement parallel to the strike of a fault (KB′ in Fig. 1; Groshong, 1999). Therefore, the fault separation has some different features from the fault slip. For example, two non-parallel markers will produce different separations (Fig. 2).

Traditionally, authors use a series of structural elements to define the fault slip including: (1) slickenside lineations or other kinematic indicators on a fault plane, (2) the geometry of the fault, (3) kinematic indicators in the damaged region within the wall-rocks, and (4) displaced lines, such as fold hinge lines (e.g., Hills, 1963; Dennis, 1972; Billings, 1972; Suppe, 1985; Ramsay and Huber, 1987; Doblas et al., 1997a,b). Recently, new methods using restoration techniques have been proposed to determine finite fault slips (e.g., Rouby et al., 2000). Those techniques require that the faults formed

* Corresponding author. Tel.: +52 55 9175 6470.
E-mail addresses: xshunshan@yahoo.com, sxu@imp.mx (S.-S. Xu).

0191-8141/$ - see front matter © 2007 Elsevier Ltd. All rights reserved.
doi:10.1016/j.jsg.2007.06.003

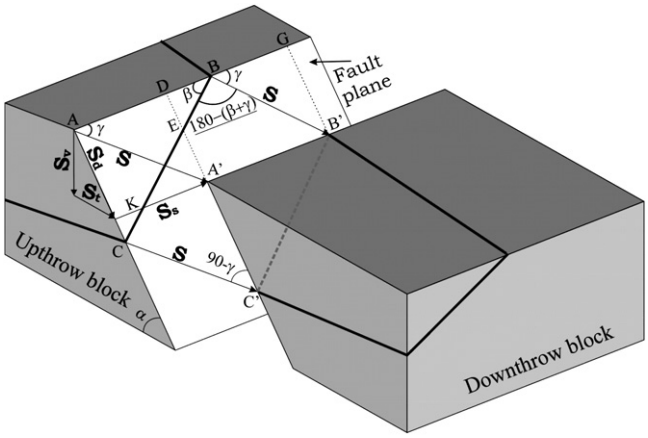

Fig. 1. Block diagram showing a marker (thick black lines) displaced by a lateral-normal-slip fault. S, slip; S_d, dip-slip; S_t, true heave; S_v, vertical component of the slip (true throw); S_s, strike-slip component; γ, pitch angle of the slip; β, pitch angle of the cutoff of the marker; $EC' = S_{md}$, dip separation; and $KB' = S_{mh}$, strike separation.

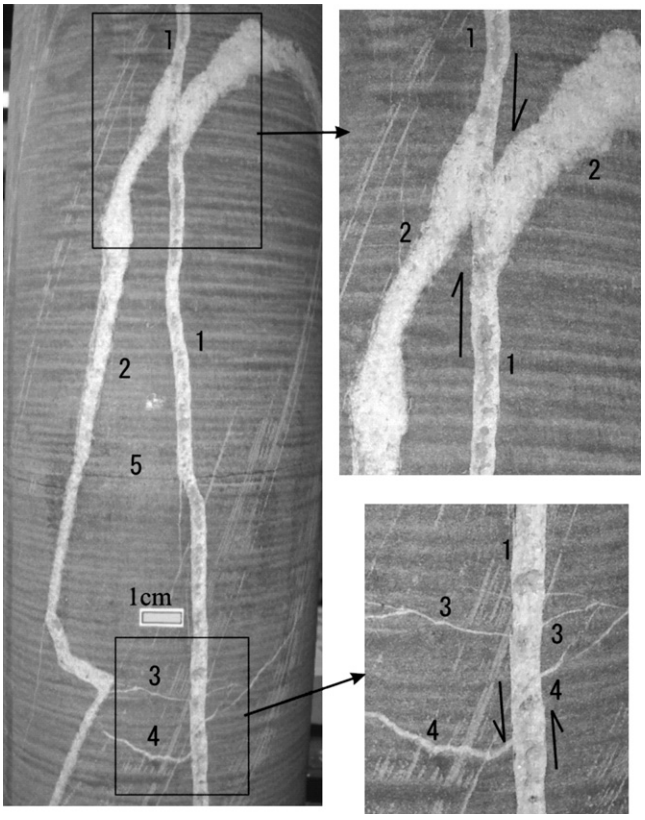

Fig. 2. Photograph of a core segment from an Upper Jurassic carbonate sequence from the Campeche Bay area (Gulf of Mexico). Two generations of calcite veins are observed; vein 1 is the second generation of veins and cuts veins 2, 3, and 4 which represent the first vein generation. Marker 5 is a lamination line parallel to the veins 3. Vein 2 shows a normal sense of displacement cut by vein 1. Vein 4 shows a reverse sense of displacement cut by vein 1. Vein 3 and the lamination line (plane) show no displacement cut by vein 1. These features indicate that vein 1 was filled in a small fault with a net slip parallel to the planes of vein 3 and the marker 5.

before or during folding (e.g., Kerr et al., 1993). Xu et al. (2004b) proposed some approaches to estimate the strike or vertical slip on a fault using structural contour maps, which are appropriate for faults that formed after folding. These methods need more assumptions and can only be applied to cases at mid-large scales, compared with the approaches that we introduce here.

In this paper, several approaches are proposed to estimate quantitatively the fault slip using fault separation. We consider two different scenarios according to different types of data that may be available. In the first situation, the fault separation and slickenside lineations on or near a fault are known; therefore, the magnitude of net slip can be estimated. The methods applied in this case are not appropriate for reactivated faults, because slickenside lineations preferentially tend to record the final slip events. In the second situation, when slickenside lineations are absent or are not observed but the fault separations for two markers are known, the fault slip direction can be determined. This approach is suitable for reactivated faults, because the evaluated slip direction shows general, but not the last, direction of the fault movement. The approaches in the two scenarios have some of the following advantages.

(1) The two methods can be applied to faults at any scale. This is appropriate to small-scale faults if displaced fold hinges are lacked, and also to large-scale fault bends in which the fault plane is difficult to observe in the field.
(2) Compared with the techniques of Xu et al. (2004b), three following conditions are not necessary: (a) structural contours; (b) the intersection angle between the fault strike and the strike of bedding is greater than 65°; and (c) the bed dip is more than 35°.

The approaches were tested on: (1) a strike-slip fault in East Quantoxhead, United Kingdom; (2) an example from the Jordan field, Ector County, Texas, and (3) a domino fault system from the Sierra de San Miguelito, central Mexico.

2. Parameters considered for estimation of fault slip

The fault separation depends not only on the attitude of the displaced marker but also on the direction and magnitude of the fault slip. For the estimation of the slip component, three parameters should be considered: (1) the pitch of slip lineation (γ); (2) the pitch (β) of a cutoff of a marker (bed, vein, etc.); and (3) the separation (S_{md} or S_{mh}) observed on the fault plane. In addition, different combinations between the fault slip and cutoffs should be considered. First, two relationships exist between the pitch direction of fault slips and the pitch direction of cutoffs; consequently, opposite and same direction of both slip and pitch direction will produce different effects on separations. Second, the dip and the strike of the fault separation need to be observed on cross-sections and map views, respectively; therefore, different equations should be applied to determine the fault slip. Third, when the pitch direction of the fault slip is the same as that of cutoff, a factor to consider is a relative pitch value between the fault slip and cutoff. In

the following section, the different scenarios mentioned above are analyzed and discussed.

Here, we give some principles to determine whether a slickenside striation and a marker trace on the fault have the same or opposite pitch direction. The dip direction of fault (P_1), the plunge direction of striation (P_2), and the dip direction of the marker (P_3) should be known. Then, we can evaluate the intersection angles among P_1, P_2, and P_3 from the dip direction of the fault. We define that the acute intersection angles from P_1 to P_2 is λ_1, and the intersection angles from P_1 to P_3 is λ_2, and positive value for clockwise (Fig. 3). Criteria to determine the pitch of a slickenside striation or a marker trace are given as follows.

(1) For $\lambda_1 < 0°$ (Fig. 3a), if λ_2 ranges from 0° to 180° or from −180° to −360° (Fig. 3b), then the striations and marker traces have opposite pitch direction; whereas if λ_2 ranges from 180° to 360° or from 0° to −180°, the slickenside striations and marker traces have the same pitch direction.
(2) For $\lambda_1 > 0°$ (Fig. 3c), if λ_2 ranges from 0° to 180° or from −180° to −360° (Fig. 3d), then the striations and marker traces have the same pitch direction; whereas if λ_2 ranges from 180° to 360° or from 0° to −180°, the striations and marker traces have opposite pitch direction.

If only the azimuth of striations on a fault is known, the pitch of the slickenside striations (β) can be evaluated. We consider three cases to calculate the value of β (Appendix A): (a) the bed or other markers is vertical, whereas the fault is not vertical; (b) the marker is inclined, whereas the fault is vertical; and (c) both the marker and the fault are inclined. The last situation is more usual.

3. Evaluation of the magnitude of fault slip

Estimation of the magnitude of total slip requires two originally contiguous points displaced by faulting. For instance, let us consider points A and A′ in Fig. 1, the magnitude of net slip is expressed by S, which has a pitch γ and can be resolved into two perpendicular components on the fault plane, that is, S_d and S_s (Fig. 1). S_s is the strike-slip component of the fault displacement and can be written as:

$$S_s = S\cos\gamma \tag{1}$$

where γ is the pitch angle of the fault slip.

S_d is the dip-slip component of the fault displacement and can be expressed as:

$$S_d = S\sin\gamma \tag{2}$$

S_d can be resolved for S_v and S_t, where S_v is the vertical component of the dip-slip (true throw) and can be calculated by:

$$S_v = S_d\sin\alpha = S\sin\gamma\sin\alpha \tag{3}$$

where α is the dip angle of the fault plane.

The horizontal component of the dip-slip (S_t) is the true heave, and can be estimated by:

$$S_t = S_d\cos\alpha = S\sin\gamma\cos\alpha \tag{4}$$

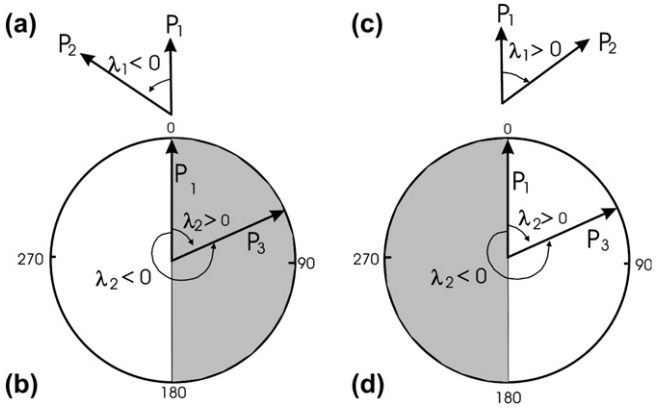

Fig. 3. Sketch map to determine the relationship between a slickenside striation and a maker trace on a fault. In (b) and (d), the shade semicircle indicates that the striations and marker trace have opposite pitch direction, and the white semicircle indicates that the striations and marker trace have the same pitch direction.

3.1. Slickenside striations with opposite pitch direction to marker traces

3.1.1. Case of a vertical cross-section perpendicular to the fault strike

In a cross-section, if the pitch of slip lineations (γ), the pitch of cutoffs (β), and the dip separation (S_{md}) are observed, then the magnitude of the fault slip can be estimated. In Fig. 1, for triangle CEC′, by using the Law of Sines, we obtain:

$$CC'/\sin(90-\beta) = EC'/\sin(\gamma+\beta) \tag{5}$$

Since $CC' = S$ and $EC' = S_{md}$, then:

$$S = EC'\frac{\sin(90-\beta)}{\sin(\gamma+\beta)} = S_{md}\frac{\sin(90-\beta)}{\sin(\gamma+\beta)} = S_{md}\frac{\cos\beta}{\sin\gamma\cos\beta+\cos\gamma\sin\beta} = S_{md}\frac{1}{\sin\gamma+\cos\gamma\tan\beta} \tag{6}$$

Therefore, S_s, S_d, S_v and S_t can be calculated according to Eqs. (1), (2), (3), and (4), respectively. For example, the dip-slip component S_d can be written as:

$$S_d = S\sin\gamma = S_{md}\frac{\sin\gamma}{\sin\gamma+\cos\gamma\tan\beta} = \frac{S_{md}\tan\gamma}{\tan\gamma+\tan\beta} \tag{7}$$

From Eq. (6), we can see that the total slip (S) is dependent upon the values of γ, β, and S_{md}. Given different values of γ, β, and S_{md}, the total slip (S) is larger than, less than, or equal to the dip separation (S_{md}) (Fig. 4a, b). In the case of $\beta > 45°$, for any value of γ, the value of S is less than S_{md} (here S_{md} is assumed to be equal to 100). In addition, the value of S has a negative relationship with the value of β (Fig. 4a). In Fig. 4b, for a small value of γ the value of S has a negative relationship, and for a large value of γ, the value of S has a positive relationship. The inflection point between the negative

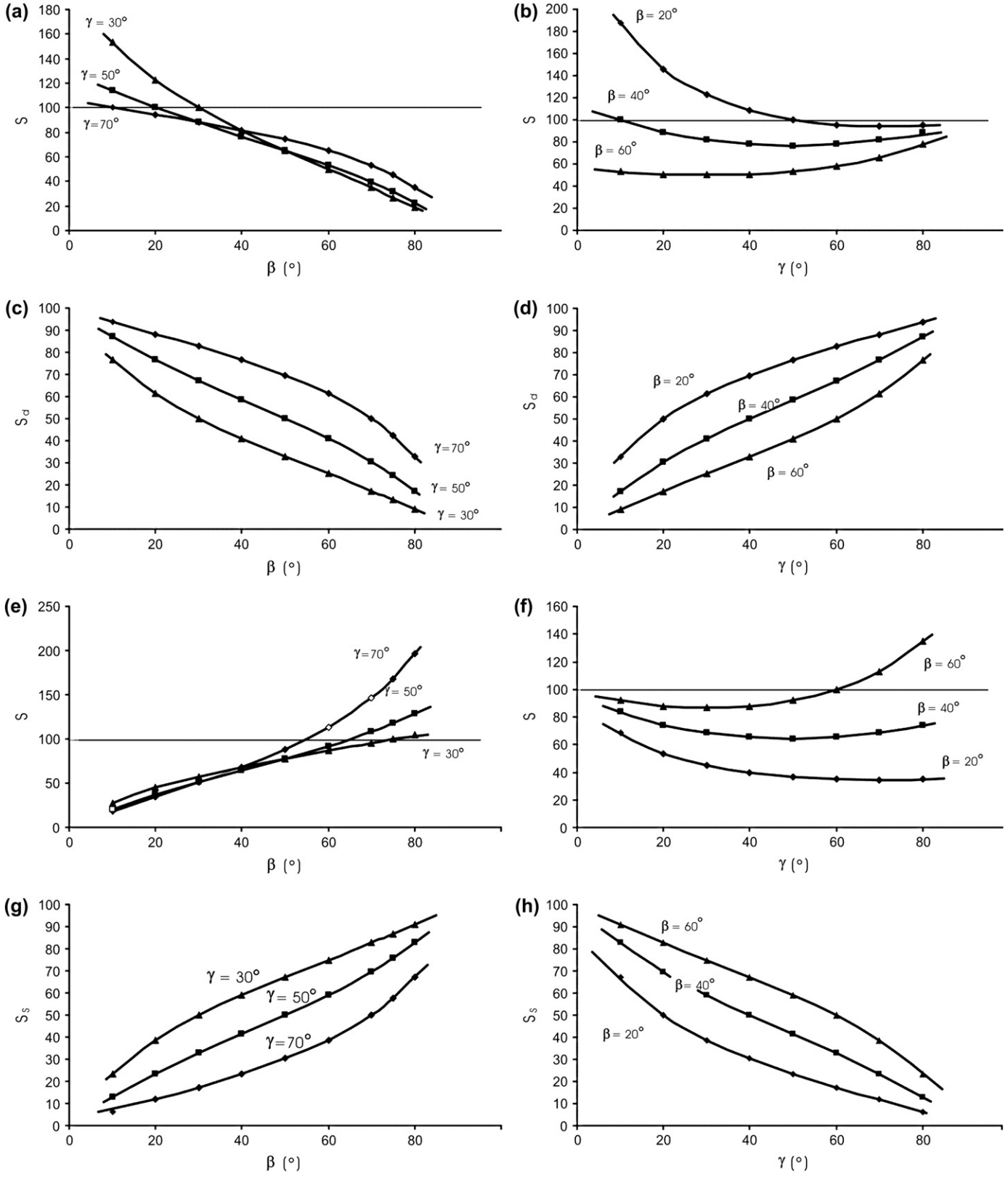

Fig. 4. Changes of the values of S, S_d and S_s in the case of slickenside striations with opposite pitch direction to marker traces (see text for details). (a) Curves show the relationship between S and β, given $\gamma = 30°$, 50°, and 70°, respectively, and $S_{md} = 100$. Data were calculated according to Eq. (6). (b) Relationship between S and γ, given $\beta = 20°$, 40°, and 60°, and $S_{md} = 100$. Data were calculated from Eq. (6). (c) Relationship between S_d and β, given $\gamma = 30°$, 50°, and 70°, and $S_{md} = 100$. Data were based on Eq. (7). (d) Changes of S_d with γ, given $\beta = 20°$, 40°, and 60°, and $S_{md} = 100$. Data were evaluated from Eq. (7). (e) Relationship between S and β according to Eq. (9), given $\gamma = 30°$, 50°, and 70°, and $S_{mh} = 100$. (f) Relationship between S and γ based on Eq. (9), given $\beta = 20°$, 40°, and 60°, respectively, and $S_{mh} = 100$. (g) Relationship between S_s and β according to Eq. (10), given $\gamma = 30°$, 50°, and 70°, and $S_{mh} = 100$. (h) Relationship between S_s and γ based on Eq. (10), given $\beta = 20°$, 40°, and 60°, and $S_{mh} = 100$.

and positive relationships depends on the value of β (Fig. 4b). From Eq. (7), given the values of γ, β, and S_{md}, the dip-slip (S_d) is always less than dip separation (S_{md}) (Fig. 4c, d). This indicates that for the case in which slickenside striations and marker traces have opposite pitches, an observed dip separation (S_{md}) overestimates the dip-slip (S_d).

3.1.2. Case of a map view

On a map view (Fig. 1), the strike separation (S_{mh}) is equal to KB′ and can be directly measured. If other data such as the pitch of slip lineations (γ) and the pitch of cutoffs (β) are known (Fig. 1), then the magnitude of the fault slip can be estimated. For triangle BKB′, by using the Law of Sines, we obtain:

$$S/\sin\beta = \mathrm{KB}'/\sin[180-(\beta+\gamma)] \tag{8}$$

Simplifying, we obtain:

$$S = \frac{S_{mh}\sin\beta}{\sin(\beta+\gamma)} = \frac{S_{mh}\tan\beta}{\tan\beta\cos\gamma+\sin\gamma} \tag{9}$$

Then parameters S_s, S_d, S_v and S_t can be calculated according to Eqs. (1), (2), (3), and (4), respectively. For instance, strike-slip component (S_s) can be written as:

$$S_s = S\cos\gamma = \cos\gamma\frac{S_{mh}\tan\beta}{\tan\beta\cos\gamma+\sin\gamma} = \frac{S_{mh}\tan\beta}{\tan\beta+\tan\gamma} \tag{10}$$

From Eq. (9), the total slip (S) is related to values of the parameters γ, β, and S_{mh}. The total slip (S) is larger than, less than, or equal to the strike separation (S_{mh}) depending on the values of γ and β (Fig. 4e, f). However, in the case of $\beta < 45°$, for any value of γ, the value of S is less than S_{mh} (Fig. 4f). In addition, the value of S has a positive relationship with the value of β (Fig. 4e). In Fig. 4f, for a small value of γ, S has a negative relationship, and for a large value of γ, S has a positive relationship. The inflection point between the negative and positive relationships depends on the value of β (Fig. 4f). From Eq. (10), given the values of γ, β, and S_{mh}, the calculated strike component of displacement (S_s) is always less than strike separation (S_{mh}) (Fig. 4g, h). This indicates that if the strike separation (S_{mh}) is regarded as the strike component of displacement (S_s), the value of (S_s) will be overestimated.

3.2. Slickenside striations with the same pitch direction as marker traces

3.2.1. Case where $\beta > \gamma$

In a vertical cross-section perpendicular to the fault strike, if the values of γ, β and S_{md} are known (Fig. 5a), we can infer equations to calculate fault slip. For triangle CEC′, by using the Law of Sines, we obtain:

$$\mathrm{CC}'/\sin(90-\beta) = \mathrm{EC}'/\sin(\beta-\gamma) \tag{11}$$

Because $\mathrm{CC}' = S$ and $\mathrm{EC}' = S_{md}$, then:

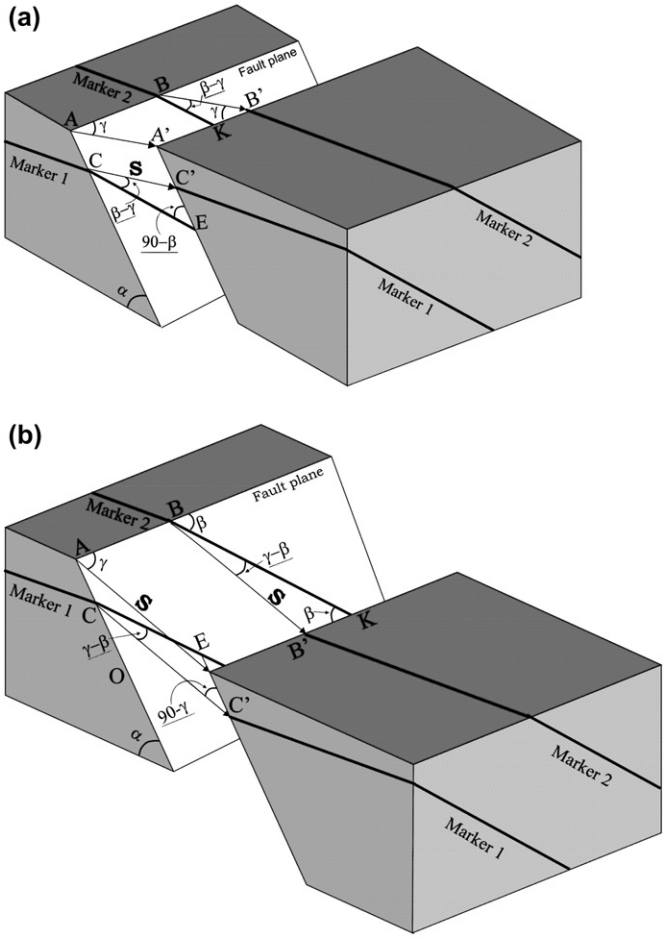

Fig. 5. Diagrams showing two parallel markers (thick black lines) displaced by a fault with a lateral-normal slip and the same pitch direction of the net slip as that of the cutoffs. EC′ is the dip separation (S_{md}). KB′ is the strike separation (S_{mh}). (a) Case where $\beta > \gamma$; the cross-section shows a reverse displacement. (b) Case where $\beta < \gamma$; the cross-section shows an apparent normal displacement.

$$S = \mathrm{EC}'\frac{\sin(90-\beta)}{\sin(\beta-\gamma)} = S_{md}\frac{\cos\beta}{\sin(\beta-\gamma)}$$
$$= S_{md}\frac{\cos\beta}{\sin\beta\cos\gamma-\cos\beta\sin\gamma} = S_{md}\frac{1}{\cos\gamma\tan\beta-\sin\gamma} \tag{12}$$

From Eqs. (1), (2), (3) and (4), we can obtain S_s, S_d, S_v and S_t, respectively. For example, S_d can be calculated by:

$$S_d = S\sin\gamma = S_{md}\frac{\sin\gamma}{\cos\gamma\tan\beta-\sin\gamma} = \frac{S_{md}\tan\gamma}{\tan\beta-\tan\gamma} \tag{13}$$

From Eqs. (12) and (13), we can compare the values between S and S_{md}, and between S_d and S_{md}. Fig. 6a, b shows that both the values of S and S_d can be larger than, less than, or equal to dip separation (S_{md}) depending on the values of γ and β and have negative relationships with the value of β.

For a map view, if the pitch angle of slip lineations (γ), the pitch angle of cutoffs (β), and the strike separation (S_{mh}) are known (Fig. 5a); then the magnitude of the fault slip can be calculated. For triangle BKB′, by using the Law of Sines, we obtain:

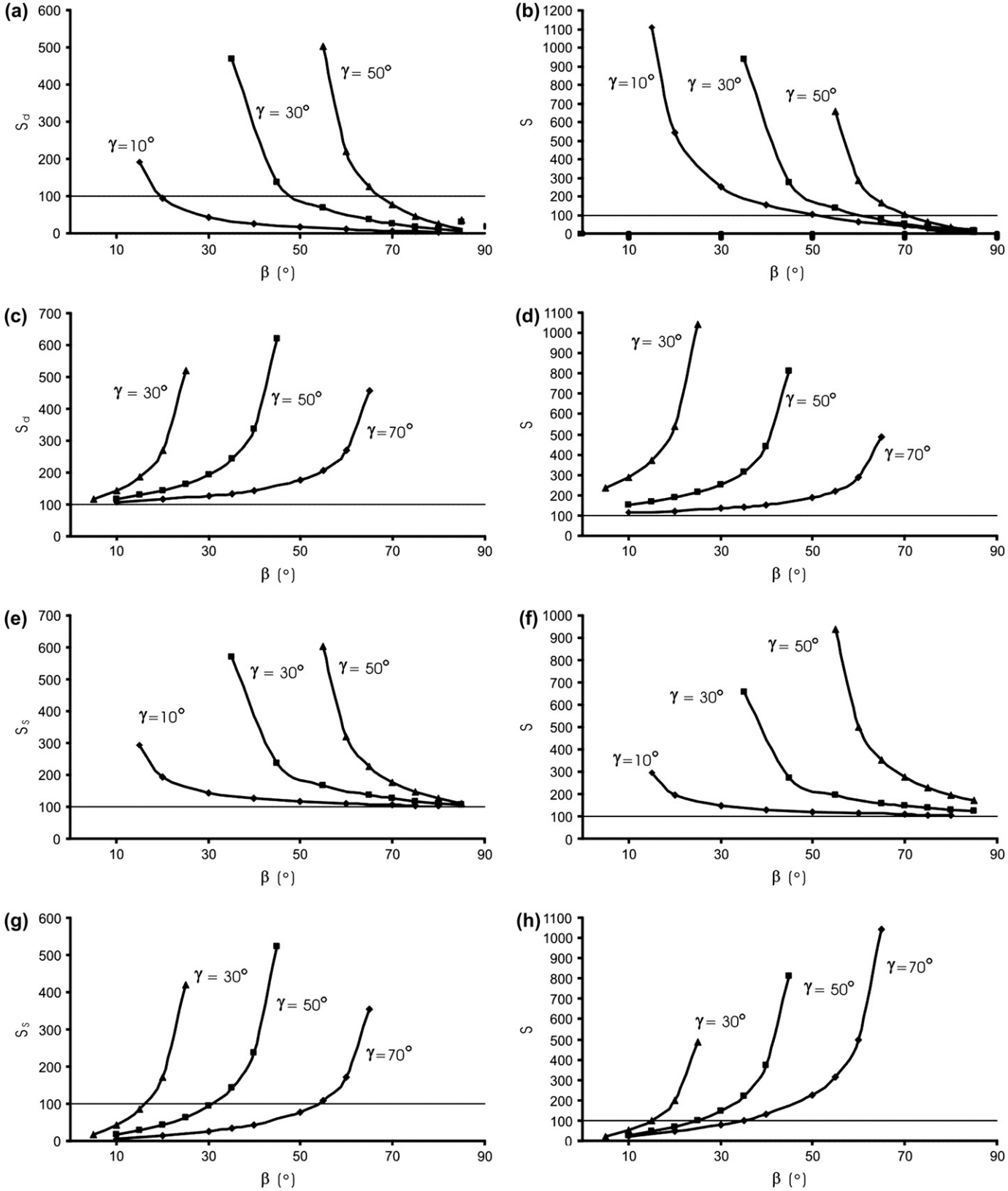

Fig. 6. Changes of the values of S, S_d and S_s in the case of slickenside striations with the same pitch direction as marker traces (see text for details). (a) Relationship between S_d and β, given $\gamma = 10°$, 30°, and 50°, and $S_{md} = 100$. Data were calculated from Eq. (13). (b) Changes of the value of S with the value of β, given $\gamma = 10°$, 30°, and 50°, and $S_{md} = 100$. Data were based on Eq. (12). (c) Curves show the relationship between S_d and β, given $\gamma = 30°$, 50°, and 70°, and $S_{md} = 100$. Data were evaluated from Eq. (19). (d) Curves show the relationship between S and γ, given $\beta = 30°$, 50°, and 70°, and $S_{md} = 100$. Data were from Eq. (18). (e) Relationship between S_s and β, given $\gamma = 10°$, 30°, and 50°, and $S_{mh} = 100$. Data are obtained from Eq. (16). (f) Relationship between S and β, given $\gamma = 10°$, 30°, and 50°, respectively, and $S_{mh} = 100$. Data were calculated according to Eq. (15). (g) Relationship between S_s and β, given $\gamma = 30°$, 50°, and 70°, and $S_{mh} = 100$. Data were based on Eq. (22). (h) Relationship between S and β, given $\gamma = 30°$, 50°, and 70°, and $S_{mh} = 100$. Data were evaluated from Eq. (21).

$$S/\sin(180-\beta) = KB'/\sin(\beta-\gamma) \quad (14)$$

Simplifying, then:

$$S = \sin\beta\frac{S_{mh}}{\sin(\beta-\gamma)} = \frac{S_{mh}}{\tan\beta\cos\gamma - \sin\gamma} \quad (15)$$

Substituting Eq. (15) into Eqs. (1)–(4), S_s, S_d, S_v and S_t can be calculated. S_s is, therefore, expressed by:

$$S_s = S\cos\gamma = \cos\gamma\frac{S_{mh}\tan\beta}{\tan\beta\cos\gamma - \sin\gamma} = \frac{S_{mh}\tan\beta}{\tan\beta - \tan\gamma} \quad (16)$$

Then, given the values of S_{mh}, β, and γ, we can calculate the values of S and S_s from Eqs. (15) and (16), respectively. The results show that the values of both S_s and S are always larger than the value of S_{mh} (Fig. 6e, f) and have negative relationships with the value of β. This means that if the strike separation (S_{mh}) is substituted for the strike-slip component (S_s), or total slip (S), the value of S_s and S will be underestimated.

3.2.2. Case where $\beta < \gamma$

Let us consider a vertical cross-section perpendicular to the fault strike where the values of γ, β and S_{md} are known (Fig. 5b). For triangle CEC′, by using the Law of Sines, we obtain:

$$CC'/\sin(90+\beta) = EC'/\sin(\gamma-\beta) \quad (17)$$

Because $CC' = S$ and $EC' = S_{md}$, then:

$$S = EC'\frac{\sin(90+\beta)}{\sin(\gamma-\beta)} = S_{md}\frac{\cos\beta}{\sin(\gamma-\beta)} = S_{md}\frac{1}{\sin\gamma - \cos\gamma\tan\beta} \quad (18)$$

Therefore, S_d, S_s, S_v and S_t can be calculated by substituting Eq. (18) into Eqs. (1), (2), (3) and (4), respectively. In this way, S_d is obtained from the following equation.

$$S_d = S\sin\gamma = \frac{S_{md}\sin\gamma}{\sin\gamma - \cos\gamma\tan\beta} = \frac{S_{md}\tan\gamma}{\tan\gamma - \tan\beta} \quad (19)$$

Then, by using different values of S_{md}, β, and γ, we can obtain the values of S and S_d from Eqs. (18) and (19), respectively. The results show that the values of both S_d and S are always larger than the value of S_{md} (Fig. 6c, d) and have a positive relationship with the value of β. From these results, we can infer that if the dip separation (S_{md}) is substituted for the dip-slip (S_d), or the total slip (S), the value of (S_d) and (S) will be underestimated.

On a map view (Fig. 5b), $KB' = S_{mh}$, for triangle BKB′, by using the Law of Sines, the following relationship can be deduced:

$$S/\sin\beta = KB'/\sin(\gamma-\beta) \quad (20)$$

Simplifying, we obtain:

$$S = \sin\beta\frac{S_{mh}}{\sin(\gamma-\beta)} = \frac{S_{mh}\tan\beta}{\sin\gamma - \tan\beta\cos\gamma} \quad (21)$$

The values of S_d, S_s, S_v and S_t can be calculated by substituting Eq. (21) into Eqs. (1), (2), (3), and (4), respectively. For example, S_s is evaluated by:

$$S_s = S\cos\gamma = \cos\gamma\frac{S_{mh}\tan\beta}{\sin\gamma - \tan\beta\cos\gamma} = \frac{S_{mh}\tan\beta}{\tan\gamma - \tan\beta} \quad (22)$$

From Eqs. (21) and (22), we can analyze the relationship between S and S_{mh}, and between S_s and S_{mh}. It can be seen in Fig. 6g, h that both the values of S and S_s can be larger than, less than, or equal to strike separation (S_{mh}) depending on the values of γ and β and have a positive relationship with the value of β.

For faults with lateral-reverse slips, the separations will show the similar effects as for faults with lateral-normal slips for the same cases. For instance, if the striations and marker traces have opposite pitch direction, the same procedure for the estimation of slip magnitudes can be carried out from the illustration of Fig. 7. Let us consider Fig. 7 where the pitch angle of the slickenlines (γ), the pitch angle of cutoffs (β), and the dip separation (S_{md}) are known. For triangle CEC′, by using the Law of Sines, we obtain:

$$CC'/\sin(90-\beta) = EC'/\sin(\gamma+\beta) \quad (23)$$

Since $CC' = S$ and $EC' = S_{md}$, then:

$$S = EC'\frac{\sin(90-\beta)}{\sin(\gamma+\beta)} = S_{md}\frac{\sin(90-\beta)}{\sin(\gamma+\beta)} = S_{md}\frac{\cos\beta}{\sin\gamma\cos\beta + \cos\gamma\sin\beta} = S_{md}\frac{1}{\sin\gamma + \cos\gamma\tan\beta} \quad (24)$$

Eq. (24) is the same as Eq. (6). Similarly, if data from a map view are known (Fig. 7), we can deduce the magnitude of the total slip S with the following equation.

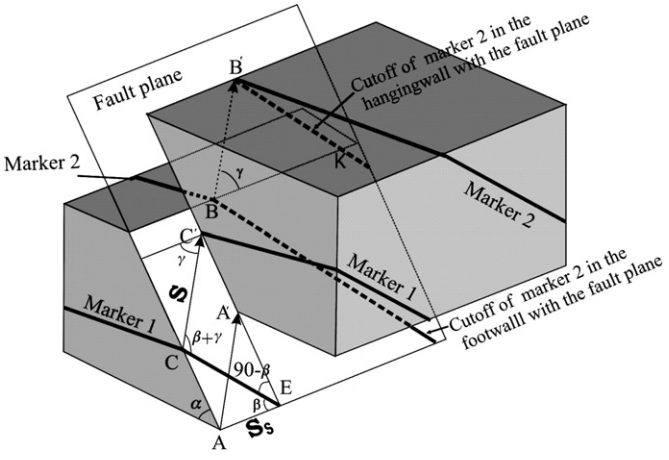

Fig. 7. Block diagram showing two parallel markers (thick black lines) displaced by a lateral-reverse fault. The pitch direction of the net slip is opposite to that of the cutoff. EC′ is the dip separation (S_{md}). KB is the strike separation (S_{mh}).

$$S = \frac{S_{mh}\tan\beta}{\tan\beta\cos\gamma + \sin\gamma} \tag{25}$$

Note that Eq. (25) is the same as Eq. (9).

When fault striations and marker traces have the same pitch direction, the cases where $\beta > \gamma$ and $\beta < \gamma$ show different effects on separations. For these cases, the magnitude of the slip can also be estimated. For simplicity, the process for deducing the equations is not repeated.

4. Evaluation of the pitch angle of slip

When slickenlines, striations and slip-fiber lineations on fault planes are absent, determining the direction of the fault slip is difficult. Therefore, before proceeding with any calculation, it is necessary to determine the fault type. The fault separations can be utilized to identify the fault type. For lateral-normal faults, if the sense of displacement of one marker is reverse, it can be deduced that the pitch direction of the slip is the same as that of the cutoff and that $\beta > \gamma$ (Fig. 5a). In contrast, if the sense of displacement of one marker in a cross-section is normal but the sense of displacement in the map view is opposite to the pitch direction of the cutoff, then the pitch direction of the slip is the same as that of the cutoff and then $\beta < \gamma$ (Fig. 5b). Similarly, for lateral-reverse faults, if the displacement of one marker shows a normal sense, it implies that the pitch direction of the slip is the same as that of the cutoff and that $\beta > \gamma$. On the other hand, if the displacement of one marker in a cross-section displays a reverse sense but the sense of displacement in the map view is opposite to the pitch direction of the cutoff, it indicates that the pitch direction of the slip is the same as that of the cutoff and that $\beta < \gamma$. Other criteria to determine the shear sense on faults, proposed by some authors (e.g., Petit, 1987; Means, 1987; Angelier, 1994; Doblas et al., 1997a,b), are not discussed in this paper.

If there are two non-parallel markers at the same point, two sets of measured data for these two markers can be obtained. Then, the pitch value (γ) of the slip can be estimated employing the two data sets. The attitudes of two marker horizons have many combinations that define which equations can be used to evaluate the pitch value of slip. For instance, if the two marker horizons are consistent with the prerequisite of Eq. (6) in the case of a cross-section view, then this equation can be used to calculate the value of γ. Thus, the following relationship can be established:

$$S_{md1}\frac{1}{\sin\gamma + \cos\gamma\tan\beta_1} = S_{md2}\frac{1}{\sin\gamma + \cos\gamma\tan\beta_2} \tag{26}$$

where S_{md1} and S_{md2} are the dip separations of the two indicators, respectively; whereas, β_1 and β_2 are the pitch angles of the cutoffs of the two indicators.

Rearranging and simplifying, we obtain:

$$\tan\gamma = \frac{S_{md2}\tan\beta_1 - S_{md1}\tan\beta_2}{S_{md1} - S_{md2}}$$

Then:

$$\gamma = \arctan\left(\frac{S_{md2}\tan\beta_1 - S_{md1}\tan\beta_2}{S_{md1} - S_{md2}}\right) \tag{27}$$

Similarly, in a map view, if the prerequisites of two indicators are consistent with Eq. (9), it can be used to estimate the pitch value of the net slip. The following relationship can be established:

$$\frac{S_{mh1}\tan\beta_1}{\tan\beta_1\cos\gamma + \sin\gamma} = \frac{S_{mh2}\tan\beta_2}{\tan\beta_2\cos\gamma + \sin\gamma} \tag{28}$$

Simplifying,

$$\tan\gamma = \frac{\tan\beta_1\tan\beta_2(S_{mh2} - S_{mh1})}{\tan\beta_1 S_{mh1} - \tan\beta_2 S_{mh2}}$$

$$\gamma = \arctan\left(\frac{\tan\beta_1\tan\beta_2(S_{mh2} - S_{mh1})}{\tan\beta_1 S_{mh1} - \tan\beta_2 S_{mh2}}\right) \tag{29}$$

If we know the dip separation of one marker (e.g., marker 1) and the strike separation of another marker (e.g., marker 2) at a place, and marker 1 is consistent with the case of Eq. (6) and marker 2 is also consistent with the case of Eq. (15), then combining these two equations the following relationship can be obtained:

$$S_{md}\frac{1}{\sin\gamma + \cos\gamma\tan\beta} = \frac{S_{mh}\tan\beta}{\tan\beta\cos\gamma - \sin\gamma}$$

Simplifying,

$$\gamma = \arctan\left(\frac{S_{md}\tan\beta - S_{mh}\tan^2\beta}{\tan\beta S_{mh} + S_{md}}\right) \tag{30}$$

Other combinations between two markers may exist, but are not discussed here.

5. Examples

In this section, applications of the quantitative approaches discussed above are illustrated. The first example is from a strike-slip fault system at East Quantoxhead, UK, published by Peacock and Sanderson (1995). In Fig. 8a, near the center of fault A, the dip separation (15 mm), the strike separation (20 mm), and the fault attitude (179°/83°E) are known. Calculated by the contours of the bed, the attitude of the bed is 83°/13°N. Using a stereonet, it can be determined that the cutoff of the bed pitches 12.8° northward (Fig. 8b). According to plunge data of slickenlines from Peacock and Sanderson (1995), the slip of this type of faults pitches approximately 15° southward. Thus, the magnitude of total slip (S) can be calculated with Eq. (6). Substituting $S_{md} = 15$, $\gamma = 15°$, and $\beta = 12.8°$ into Eq. (6), then $S = 31$ mm. Therefore, $S_d = S\tan\gamma = 8.3$ mm, and $S_s = S\,\mathrm{ctan}\,\gamma = 115$ mm. These results indicate that the strike-slip (115 mm) of fault A is much larger than the strike separation (20 mm), and that the dip-slip (8.3 mm) is smaller than the dip separation (15 mm). The fact that the strike-slip be greater than dip-slip is consistent with the observations by Peacock and Sanderson (1995).

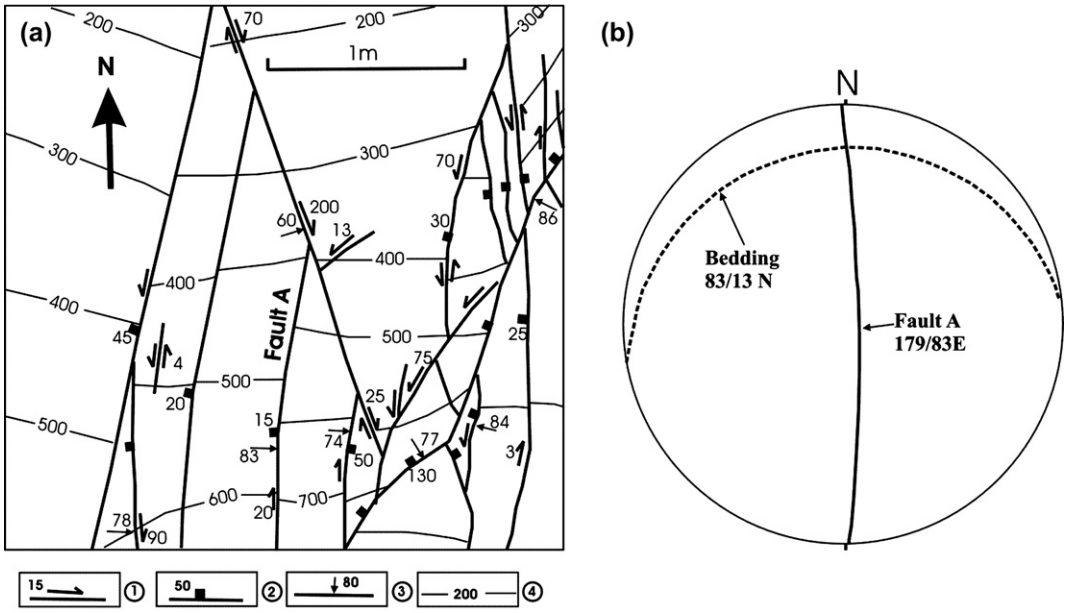

Fig. 8. (a) Structural map of a fault striking 20° NE at East Quantoxhead, UK (modified from Fig. 5c of Peacock and Sanderson, 1995). ①, Fault with a strike-slip displacement in mm; ②, fault with black square on downthrown side and downthrown in mm; ③, fault with dip angle; ④, contour in mm above an arbitrary level. (b) Equal angle projections of the bed and fault A.

The second example is from the Jordan-Penwell Ellenburger oilfield, Texas (Moody, 1973; Fig. 9). The map of structure contours shows that the oilfield is dominated by an NW–SE asymmetric anticline cut by a strike-slip fault. According to Xu et al. (2004a), the pitch of slip line on the fault is 1.4° (value of γ), the strike separation (S_{mh}) for the contour line 6100 ft is 1902.0 m. We measure that the bed angle from the contours 6100–6300 ft of the NE limb is 8.5°. Since the fault is vertical (Moody, 1973), we apply the Eq. (A8) to calculate the value of β for the bed ($\beta = 7.3°$). Since the pitch direction of slip and cutoff is the same and β is larger than γ, we can use Eq. (15) to calculate the total slip (S). Thus, the calculated value of S is equal to 2351 m. The strike-slip component (S_s) is, therefore, 2352 m. This value is closely consistent with the displacement of the fault measured from the displaced hinge line (2252.5 m) (the relative error is 4.5%).

The third example is from the Sierra de San Miguelito, central Mexico. The normal faults in this area are sub-parallel (Xu et al., 2004a). The fault traces are with strikes of 300–340°. Nearly all faults have SW dip-directions varying from 45° to 75°. The striations on fault surfaces are observed with a pitch of 70–85° (Table 1). Xu et al. (2004a) documented a vertical shear mechanism of bed tilting and obtained that the extension ratio along a cross-section (Fig. 10) nearly perpendicular to fault strikes is ca. ~0.19. For that calculation, the normal faults are assumed as dip-slip faults, e.g., the value of γ is equal to 90°. In order to test the effect of oblique slickenside striations on the calculated results of extension, here we recalculated the extension along the cross-section.

For vertical shear, the horizontal distance between the footwall cutoff of one fault and the hanging-wall cutoff in the next fault will remain constant (L_0 in Fig. 11) as deformation proceeds (Westaway and Kusznir, 1993). In this way, from Fig. 11 we obtain $DC = BC' = L_0$ and the heave is D′B. The vertical simple shear causes that the initially horizontal surface between faults to be progressively tilted by an angle θ. Thus, the present length (L_b) of the bed is AC′. Using trigonometry, we obtain:

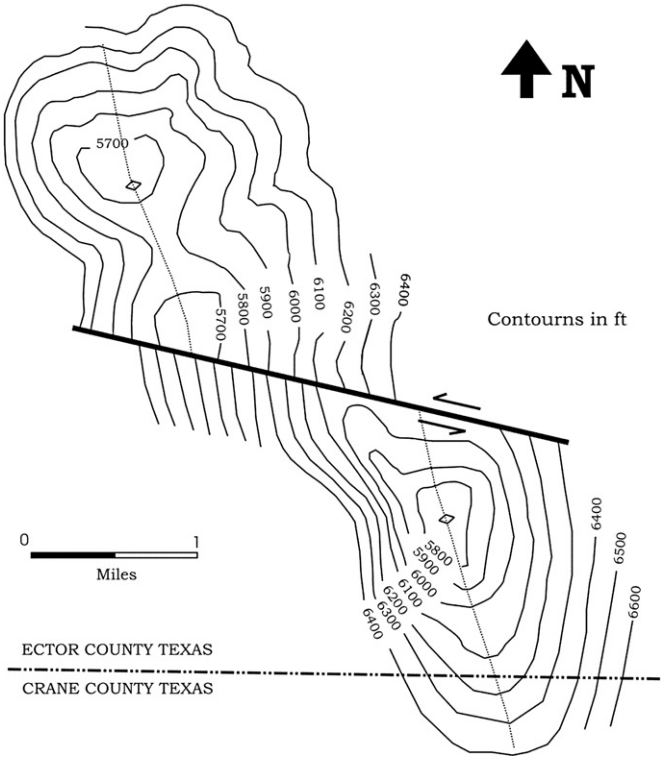

Fig. 9. Structure contour map of top of the Ellenburger formation in the Jordan field, Ector County, Texas. Modified from Moody (1973). Contours in meters below sea level.

Table 1
Data to calculate the extension due to faulting along the section in Fig. 9

No.	3	4	5	6	7	8	9	10	11	12	13	14	15
$A1/\alpha$ (°)	220/63	239/54	210/64	250/45	200/75	215/55	238/58	226/75	246/65	220/67	245/64	230/65	235/66
$A2/\theta$ (°)	16/25	30/23	20/25	31/28	42/30	48/24	25/22	30/15	30/22	10/13	46/18	35/19	38/12
γ (°)/$A3$	75SE	78SE	70SE	76SE	80NW	76NW	75SE	77SE	76SE	76SE	75SE	76SE	72SE
θ' (°)	21.1	21.7	22	26.7	29.8	24	20.1	14.1	20.8	10.0	18	18.4	11
β (°)	12.1	17.7	5.5	36.3	14.5	10	15.8	4.4	16.1	5.8	7.9	6.4	4.2
L_b (m)	660	540	500	438	755	1120	540	400	1180	550	450	1980	790
L_0 (m)	615.7	501.7	463.6	391.3	655.2	1023.2	507.1	387.9	1103.1	539.3	427.9	1878.8	773.6
S_{md} (m)	266.7	246.8	208.4	278.3	388.5	556.1	218.8	100.9	462.3	103.8	154.7	689.6	175.4
S_{mt} (m)	139	151	103	206	101	319	124	28	206	53	68	293	76
S_{ct} (m)	121.1	145.1	91.4	196.8	100.5	318.9	115.9	26.1	195.4	40.5	67.8	291.4	71.3
S_t (m)	114.5	135.8	88.2	166.3	96.1	305.6	107.8	25.7	182.3	39.5	65.4	283.5	70.1
ξ (%)	6.6	9.3	3.2	30.5	4.4	13.3	8.1	0.4	13.1	1.0	2.4	7.9	1.2
ξ' (%)	21.4	11.2	16.8	23.9	5.1	4.4	15.0	8.9	13.0	3.4	4.0	3.4	8.4

$A1$ is the dip direction of the fault. $A2$ is the dip direction of the bed. $A3$ is the pitch direction of slickenside lineations on fault. $\theta' = \arctan[\tan(\theta)\cos(\mu')]$, where μ' is the intersection angle between the cross-section direction and the bed dip direction (Xu et al., 2004a). Parameter ξ is the relative error of S_{ct}, compared to S_t. Parameter ξ' is the relative error of S_{mt}, compared to S_t. See text for definition of the parameters α, θ, γ, β, L_b, L_0, S_{md}, S_{mt}, S_{ct}, and S_t.

$$\mathrm{AB} = L_b \sin\theta \text{ and} \tag{31}$$

$$L_0 = L_b \cos\theta \tag{32}$$

From Table 1, three types of heaves are shown. The measured apparent heaves (S_{mt}) are directly measured from the cross-section. The parameter S_{ct} is the apparent heave assumed that the faults are with dip-slip striations and calculated by the equation $S_{ct} = L_b \sin(\theta')/\tan(\alpha)$, where θ' is the apparent bed dip in the direction of the cross-section.

The true heave (S_t) is calculated by the real slickenside lineations on the faults. To calculate S_t, from Fig. 11, the dip separation: $S_{md} = L_b \sin(\theta')/\sin(\alpha)$ is necessary. By using the principles in Fig. 3, we know that the pitch of the slip striations and the pitch of the cutoffs of the bed have the opposite direction. In this situation, for $\beta < \gamma$, then Eq. (18) should be used to calculate the total slip (S):

$$S = \frac{S_{md}}{\sin\gamma + \cos\gamma \tan\beta} \tag{33}$$

The dip-slip S_d is:

$$S_d = S \sin\gamma \tag{34}$$

Then, the true heave is:

$$S_t = S \sin\gamma \cos\alpha \tag{35}$$

Our results show that the true heave (S_t) is always smaller than the calculated apparent heave (S_{ct}) for all fault blocks. The errors of S_{ct} for different fault blocks show that most of relative errors are smaller than 10%, and that the largest relative error is 30.5% (Table 1). The errors of the measured heaves (S_{mt}) for different fault blocks are also calculated. In this case, the largest relative error of S_{mt} is 23.9% (Table 1). For the measured heave (S_{mt}), we use the equation $\varepsilon_{mt} = (\sum S_{mt}/\sum L_0)$ to calculate the extension due to faulting. The total extensional strain $\varepsilon_{mt} = 0.2014$. For the calculated apparent heave (S_{ct}), we use the equation $\varepsilon_{ct} = (\sum S_{ct}/\sum L_0)$. We obtained that the total extensional strain $\varepsilon_{ct} = 0.1922$. Similarly, for the true heaves, the equation $\varepsilon_t = (\sum S_t/\sum L_0)$ is used. The obtained total extensional strain of ε_t is 0.1813. According to Nieto-Samaniego et al. (1999) and Xu et al. (2004b), the extension along the direction of the studied cross-section is ca. 0.18. This value is obtained from the model of Krantz (1988) using fault slickenside lineation data. It can be seen that the extension using the true heaves (0.18213) is closer to 0.18 than that using the calculated apparent heaves (0.1922) and than that using the measured apparent heaves (0.2014).

6. Conclusions

In this paper, we have quantitatively analyzed the problem of whether the fault slip and fault separation are related to

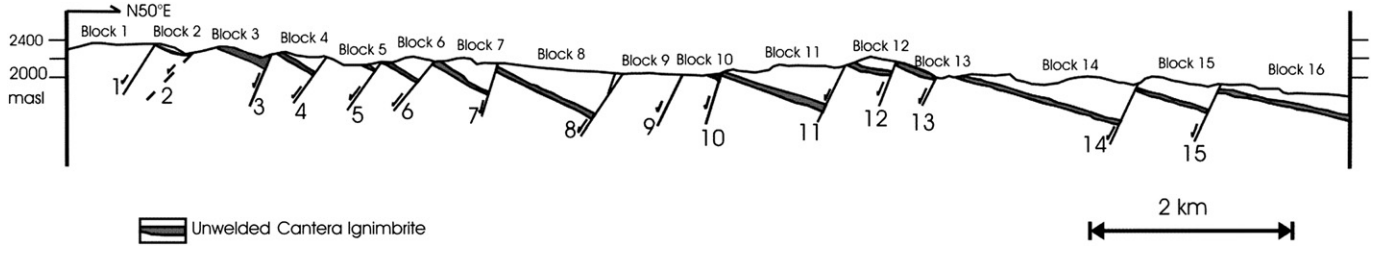

Fig. 10. Cross-section sub-perpendicular to fault strikes in the Sierra de San Miguelito. Only one bed as marker is shown. The displacements of faults 1 and 2 cannot be measured because of lack of a marker. Data for other faults are listed in Table 1. Modified from Xu et al. (2004a).

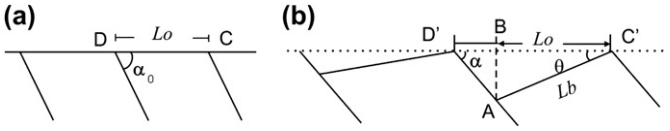

Fig. 11. Sketch to illustrate the relationships among parameters for domino faults assuming vertical shear supposed by Westaway and Kusznir (1993).

each other in geometry. The results show that the separation depends on the pitch of slip lineation (γ), the pitch of a cutoff (β), the dip separation (S_{md}) or the strike separation (S_{mh}) for one marker. The cases of cross-section and map view can be considered separately. In the case of slickenside striations with opposite pitch direction to marker traces, the dip-slip (S_d) is always less than the dip separation (S_{md}), whereas the total slip (S) is larger than, less than or equal to the dip separation (S_{md}) or strike separation (S_{mh}), depending on the combinations of the values of γ and β. In the case of slickenside striations with the same pitch direction as marker traces, two sub-cases are considered. First, for $\beta > \gamma$, the dip-slip (S_d) and total slip (S) are larger than, less than or equal to the dip separation (S_{md}) for different combinations of the values of γ and β. Nevertheless, the strike-slip component (S_s) is always larger than the strike separation (S_{mh}). Second, for $\beta < \gamma$, the dip-slip (S_d) and total slip (S) are larger than the dip separation (S_{md}) for any combinations of the values of γ and β, whereas the strike-slip component (S_s) is larger than, less than or equal to the strike separation (S_{mh}) depending on combinations of the values of γ and β. In addition, if two or more marker horizons exist at a point, we can calculate the slip direction. However, it is important to consider the type of fault before proceeding with the quantitative estimation of the slip direction.

The equations established in this study were tested in three examples. First, the calculated separations from an outcropping strike-slip fault at East Quantoxhead, United Kingdom, are consistent with the observations in the field. Second, the strike-slip component ($S_s = 2352$ m) of the strike-slip fault in the Jordan-Penwell Ellenburger oilfield, Texas is closely consistent with the displacement of the fault measured from the displaced hinge line (2252.5 m) (relative error is 4.5%). Finally, in the Sierra de San Miguelito, central Mexico, for individual fault blocks, the largest relative error of the apparent calculated heaves (S_{ct}) is 30.5%. The extension calculated from the true heaves is more nearly consistent with the published value than from the apparent heaves.

Acknowledgements

This work was supported by the research project D.01003 of the Instituto Mexicano del Petróleo. Review comments by D.C.P. Peacock are gratefully acknowledged. We also thank Steve Laubach for reviewing and improving the paper.

Appendix A.

To calculate the pitch (β) of the intersection line of a fault with an arbitrary plane (marker, bed, plunge plane of slickenside lineation, etc.), three cases are considered.

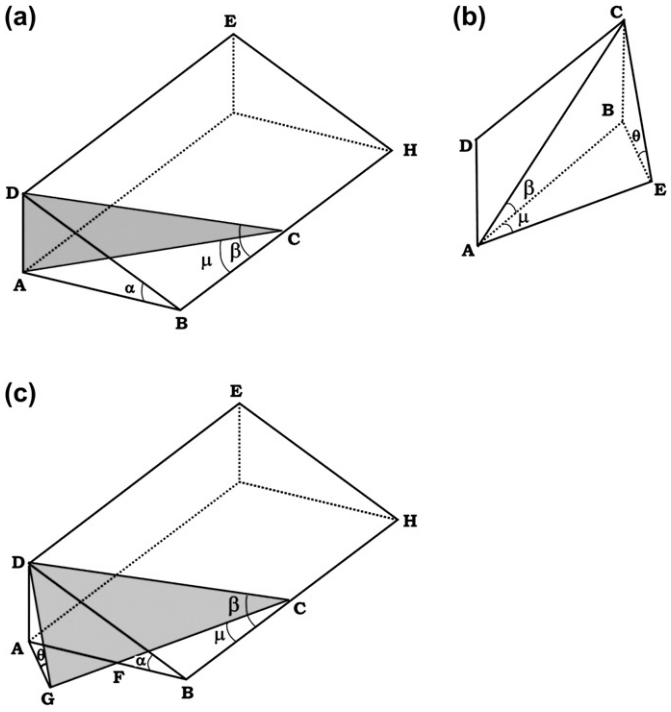

Fig. A1. Diagrams showing an arbitrary marker intersecting a fault. (a) Plane DBHE is a fault plane and plane ACD is a vertical marker. (b) Plane ABCD is a vertical fault and plane AEC is an inclined marker. (c) Plane DBHE is a fault plane and plane DGC is an inclined marker. In the diagrams, α represents the angle of the fault, θ is the angle of an arbitrary marker, μ is the acute intersection angle of the fault strike with the marker direction, and β is pitch angle of the cutoff.

First, we consider an inclined fault that intersects with a vertical plane. This is shown in Fig. A1-a. For the right triangle ABD, we obtain:

$$\mathrm{DB} = \mathrm{AD}/\sin\alpha \tag{A1}$$

$$\mathrm{AB} = \mathrm{AD}/\tan\alpha \tag{A2}$$

For the right triangle ABD, we have following equation:

$$\mathrm{BC} = \mathrm{AB}/\tan\mu = \mathrm{AD}/\tan\mu\tan\alpha \tag{A3}$$

For the right triangle ABD, we obtain:

$$\tan\beta = \mathrm{DB}/\mathrm{BC} = (\mathrm{AD}/\sin\alpha)/(\mathrm{AD}/\tan\mu\tan\alpha) \tag{A4}$$

Then:

$$\beta = \arctan(\tan\mu/\cos\alpha) \tag{A5}$$

Second, we consider a vertical fault that intersects an inclined plane. This is shown in Fig. A1-b. For the right triangle ABE,

$$BE = AB\sin\mu \tag{A6}$$

For the right angle CBE,

$$CB = BE\tan\theta = AB\sin\mu\tan\theta \tag{A7}$$

For the right angle ABC,

$$\tan\beta = CB/AB = \sin\mu\tan\theta$$

Then:

$$\beta = \arctan(\sin\mu\tan\theta) \tag{A8}$$

Third, both the plane and the fault are inclined. This is shown in Fig. A1-c. For the right triangle ADG, we deduce that,

$$AG = AD/\tan\theta \tag{A9}$$

For the right triangle AGF, we obtain:

$$AF = AG/\cos\mu = AD/\cos\mu\tan\theta \tag{A10}$$

For the right triangle ADB, we infer that,

$$AB = AD/\tan\alpha \text{ and} \tag{A11}$$

$$DB = AD/\sin\alpha \tag{A12}$$

We can evaluate value of FB according to Eqs. (A10) and (A11),

$$FB = AB - AF = AD/\tan\alpha - AD/\cos\mu\tan\theta = \frac{AD(\tan\theta\cos\mu - \tan\alpha)}{\tan\alpha\tan\theta\cos\mu} \tag{A13}$$

For the right triangle FBC, we obtain:

$$BC = FB/\tan\mu = \frac{AD(\tan\theta\cos\mu - \tan\alpha)}{\tan\alpha\tan\theta\sin\mu} \tag{A14}$$

For the right triangle DBC, we have:

$$\tan\beta = DB/BC \tag{A15}$$

Substituting Eqs. (A13) and (A14) into Eq. (A15),

$$\tan\beta = (AD/\sin\alpha)/(AD(\tan\theta\cos\mu - \tan\alpha)/ \times(\tan\alpha\tan\theta\sin\mu)) \tag{A16}$$

Simplifying Eq. (32), it can be written as:

$$\tan\beta = \frac{\sin\mu\tan\alpha\tan\theta}{\sin\alpha(\tan\theta\cos\mu - \tan\alpha)} \tag{A17}$$

Then:

$$\beta = \arctan\left(\frac{\sin\mu\tan\alpha\tan\theta}{\sin\alpha(\tan\theta\cos\mu - \tan\alpha)}\right) \tag{A18}$$

References

Angelier, J., 1994. Fault slip analysis and paleostress reconstruction. In: Hancock, P. (Ed.), Continental Deformation. Pergamaon, New York, pp. 53–100.

Bates, R.L., Jackson, J.A., 1987. Glossary of Geology, third ed. American Geological Institute, Alexandria, Virginia, 788 pp.

Billings, M.P., 1972. Structural Geology, third ed. Prentice-Hall, Englewood Cliffs, NJ, 606 pp.

Dennis, J.G., 1972. Structural Geology. Ronald Press, New York, 532 pp.

Doblas, M., Faulkner, D., Mahecha, V., Aparicio, A., Lopez-Ruiz, J., Hoyos, M., 1997a. Morphologically ductile criteria for the sense of movement of slickensides from an extensional detachment fault in southern Spain. Journal of Structural Geology 19, 1045–1054.

Doblas, M., Mahecha, V., Hoyos, M., Lopez-Ruiz, J., 1997b. Slickenside and fault surface kinematic indicators on active normal faults of the Alpine Betic cordilleras, Granada, southern Spain. Journal of Structural Geology 19, 159–170.

Groshong, R.H., 1999. 3-D Strutural Geology: A Practical Guide to Surface and Subsurface Map Interpretation. Springer-Verlag, Berlin, hardcover, xv + 324 pp.

Hill, M.L., 1959. Dual classification of faults. American Association of Petroleum Geologists Bulletin 43, 217–237.

Hills, E.S., 1963. Elements of Structural Geology. Methuen and Co., London, 483 pp.

Kerr, H., White, N., Brun, J.P., 1993. An automatic method for determining 3-dimensional normal fault geometry. Journal of Geophysical Research 98, 17837–17857.

Krantz, R.W., 1988. Multiple fault sets and three-dimensional strain: theory and application. Journal of Structural Geology 10, 225–237.

Means, W.D., 1987. A newly recognized type of slickenside striation. Journal of Structural geology 9, 585–590.

Moody, J.D., 1973. Petroleum exploration aspects of wrench-fault tectonics. Bulletin of American Association Petroleum Geologist 57, 449–476.

Nieto-Samaniego, A.F., Ferrari, L., Alaniz-Alvarez, S.A., Labarthe-Hernández, G., Rosas-Elguera, J., 1999. Variation of Cenozoic extension and volcanism across the southern Sierra Madre Occidental Volcanic Province, México. Geological Society of America Bulletin 111, 347–363.

Peacock, D.C.P., Sanderson, D.J., 1995. Strike-slip relay ramps. Journal of Structural Geology 17, 1351–1360.

Petit, J.P., 1987. Criteria for the sense of movement on fault surfaces in brittle rocks. Journal of Structural Geology 9, 597–608.

Ramsay, J.G., Huber, M.I., 1987. The Techniques of Modern Structural Geology, Volume 2: Folds and Fractures. Academic Press, London, 462 pp.

Reid, H.F., Davis, W.M., Lawson, A.C., Ransome, F.L.Committee, 1913. Report of the committee on the nomenclature of faults. Geological Society of America Bulletin 24, 163–186.

Rouby, D., Xiao, H., Suppe, J., 2000. 3-D restoration of complexly folded and faulted surfaces using multiple unfolding mechanisms. American Association of Petroleum Geologists Bulletin 84, 805–829.

Suppe, J., 1985. Principles of Structural Geology. Prentice-Hall, Englewood Cliffs, NJ, 537 pp.

Tearpock, D.J., Bischke, R.E., 2003. Applied Subsurface Geological Mapping with Structural Methods, second ed. Prentice Hall PTR, 822 pp.

Walsh, J.J., Watterson, J., 1988. Analysis of the relationship between displacements and dimensions of faults. Journal of Structural Geology 10, 239–247.

Westaway, R., Kusznir, N., 1993. Fault and bed "rotation" during continental extension: block rotation or vertical shear? Journal of Structural Geology 6, 753–770.

Xu, S.-S., Nieto-Samaniego, A.F., Alaniz-Álvarez, S.A., 2004a. Tilting mechanism in domino faults of the Sierra de San Miguelito, Central Mexico. Geologica Acta 3, 189–201.

Xu, S.-S., Velasquillo-Martinez, L.G., Grajales-Nishimura, J.M., Murillo-Muñetón, G., García-Hernández, J., Nieto-Samaniego, A.F., 2004b. Determination of fault slip components using subsurface structural contours: methods and examples. Journal of Petroleum Geology 27, 277–298.